ISSN 2078-7405 Cutting & Tools in Technological System, 2025, Edition 102

UDC 621.923.74 **doi: 10.20998/2078-7405.2025.102.07**

CARBON DIOXIDE EMISSIONS AND SURFACE ROUGHNESS ANALYSIS DURING DIAMOND BURNISHING

Szilárd **Smolnicki** [0009-0006-1535-5295], Gyula **Varga** [0000-0003-3810-2881]

University of Miskolc, 3515 Miskolc-Egyetemváros, Hungary
gyulavarga@uni-miskolc.hu

Received: 25 May 2025 / Revised: 02 June 2025 / Accepted: 09 June 2025 / Published: 20 June 2025

Abstract. *Carbon emissions are one of the most pressing environmental problems of our time.* CO_2 *emitted by human activities, especially industry, transport and energy production, is a major contributor to the gradual warming of the Earth's atmosphere. The aim of my research is to investigate the relationship between carbon dioxide emissions and surface roughness by varying different technological parameters during diamond burnishing.*
In the first chapter of this paper, we will review the current state of the art and literature on carbon dioxide emissions and then, based on a chosen methodology, we will show how carbon dioxide emissions from diamond polishing can be quantified. Following the calculation, we will present the technological parameters used for the machining, the test pieces on which we measured surface roughness after diamond burnishing, and some additional calculations needed to evaluate the data. In the main part of the research, we will evaluate the calculated data using 2D and 3D surface roughness metrics, with a special focus on the characteristics of the Abbott-Firestone curve.
Keywords: *energy efficiency; sustainable development; slide diamond burnishing; surface finish.*

1. Examination of carbon dioxide emissions

Carbon dioxide emissions are among the most pressing environmental issues of our time. Human activities – particularly in industry, transportation, and energy production – release large amounts of CO_2, significantly contributing to the gradual warming of Earth's atmosphere. While carbon dioxide (CO_2) is responsible for climate change, other substances such as carbon monoxide (CO), nitrogen oxides (NOX), and unburned hydrocarbons can be considered harmful to human health [1]. Although CO_2 is not toxic to human health on its own, its long-term accumulation poses a serious threat to the planet's climate. In the field of mechanical processing, carbon dioxide emissions can also be significant. Therefore, it is important to identify optimal processes with the right process parameters to help reduce CO_2 emissions [2].

According to the report of the International Energy Agency [3], we can observe how the increase in carbon dioxide emissions has changed over decades. The last period when emissions did not grow was after the Great Depression and

World War II. Since then, emissions have been increasing – sometimes more, sometimes less. It is also evident that major events such as the dissolution of the Soviet Union or China's rapid development can influence the emission rate: the former slowed it down, the latter accelerated it. Furthermore, the use of renewable energy sources cannot be ignored, as they reduce hydrocarbon use, and this impact is shown in the final column of Figure 1. It is evident that low carbon manufacturing has become a key expectation in industry. Therefore, quantitative analysis of energy consumption and CO_2 emissions in manufacturing processes is essential. This is what leads us from the scientific understanding of efficient production to industrial implementation [4]. A review of the literature reveals numerous efforts aimed at achieving this goal. A few of these are outlined below.

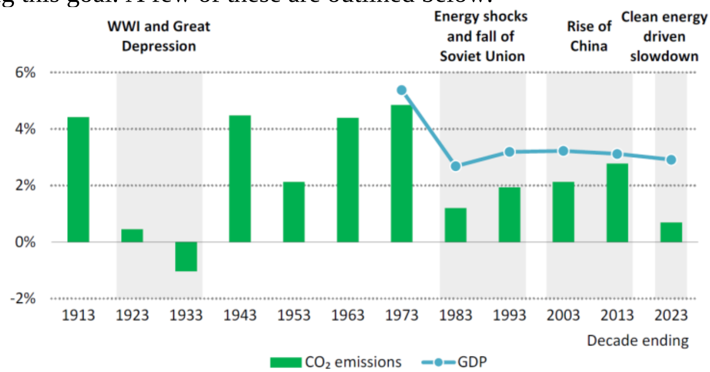

Figure 1. Global CO_2 emissions and GDP growth rate by decade [3]

Based on the operation sequence of machining, the energy consumption of machine tools can be divided into three modes—idle mode, running mode, and production mode. Various studies have focused on these distinct modes [5]. Others have found that reducing idle time and downtime helps minimize energy consumption [6]. A method has also been developed to predict total energy consumption for a specific turning operation on a machine tool [7]. Energy minimization has been analyzed using discrete statistical formulas as well [8].

Moreover, some methods directly link the electrical energy used during manufacturing to the CO_2 emissions generated during the process [9]. Others have focused on production planning problems in highly automated manufacturing systems, considering multiple process plans with different energy requirements [10]. Approaches from a mathematical standpoint have also been explored, including programming models that focus on process-level scheduling to reduce energy consumption and CO_2 emissions [11]. Research has also examined the relationship between carbon footprint and the manufacturing industry, analyzing its environmental impact [12]. An integrated concept has been published that aims to promote energy efficiency at various levels within manufacturing companies, taking into account the interdependence of all technical processes [13]. An analytical method has also been proposed to quantify the CO_2 emissions of a *CNC*-based machining system, while breaking down the processes that contribute to the system's total CO_2 emissions [14].

As seen, many approaches exist to quantify carbon dioxide emissions. In this study, a model [2] is selected for evaluating CO_2 emissions, which considers the average emissions per kilowatt-hour and the technological parameters of the machining process. In the case of diamond burnishing, these parameters include the burnishing force, burnishing speed, and feed rate.

Carbon dioxide emissions can be calculated using Equation (1):

$$CE = CE_{el} \cdot W\ [g] \tag{1}$$

Where "CE_{el}" is the carbon dioxide emission factor for electricity, which can be obtained from the EMBER database [15], available by country and year. Figure 2 shows the data filtered for Hungary, starting from the 1990s.

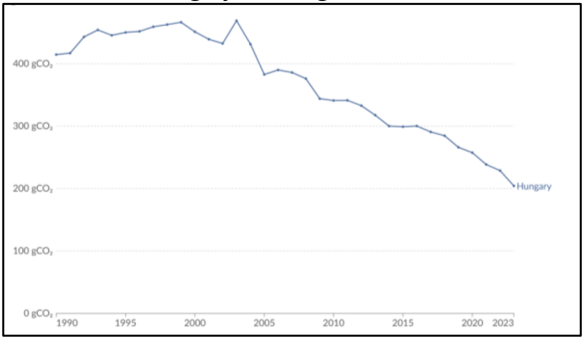

Figure 2. CO_2 emission factor of electricity in Hungary [16]

For the current calculation, the value of the carbon dioxide emission factor is:

$$CE_{el} = 229\,\frac{g}{kWh}$$

In the formula, "W " represents the energy consumption of the machining process, which can be calculated using Equation (2):

$$W = P \cdot t\ [kWh] \tag{2}$$

Here, "P" is the power requirement of the machining process, calculated using Equation (3), and "t" is the machining time, which can be calculated using Equation (4):

$$P = F \cdot v_v\ \ \left[W = \frac{N\cdot m}{s}\right] \tag{3}$$

$$t = \frac{L}{v_f} = \frac{L}{f \cdot n}\ [s] \tag{4}$$

The burnishing speed required for power calculation can be determined using Equation (5), where "n" is the rotational speed and "d" is the diameter of the test piece. In the time formula, "n" again refers to spindle speed, "L" is the length of the machining on the test piece, and "f" is the feed rate used in the process:

$$v_v = d \cdot \pi \cdot n\ \left[\frac{m}{s}\right] \tag{5}$$

The burnishing force required for the power calculation can be computed using Equation (6):

$$F = \mu \cdot F_v \tag{6}$$

Here, "μ" is the coefficient of friction, which in the case of a diamond-steel contact with cooling-lubricating fluid is μ = 0.1 [18]. Therefore, the subsequent calculations use the burnishing force multiplied by the coefficient of friction.

This burnishing force calculation is necessary because the force set as a technological parameter is passive in terms of cutting direction, while the burnishing speed in Equation (5) points in the direction of the main cutting force (as this is the cutting speed). Therefore, the set burnishing force must be converted using the friction force relationship. The spatial relationship of the forces is illustrated in Figure 3. In this case, the passive force, which can be directly set as a technological parameter during machining, is considered the normal force (denoted F_n in the figure), while the main cutting force used in the calculations is the frictional force (denoted F_s). Their relationship is shown in Equation (7), which is structurally identical to Equation (6), differing only in the notation of the forces:

$$F_s = \mu \cdot F_n \tag{7}$$

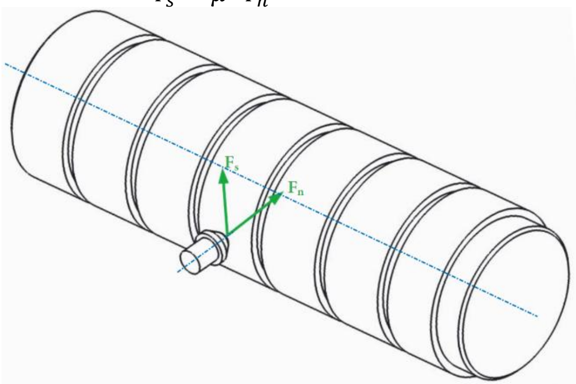

Figure 3. Spatial relationship of actual and calculated burnishing forces

Thus, for the calculation of CO_2 emissions, only the defined technological parameters, the dimensions of the test piece, and the CO_2 emission factor are needed.

2. Surface machining and roughness measurement

To perform calculations and draw conclusions with an adequate level of reliability, enough experiments must be carried out by combining technological parameters. The following values were selected for feed rate, spindle speed, and burnishing force:

$$f_1 = 0.05 \frac{mm}{rev};\ f_2 = 0.1 \frac{mm}{rev}$$

$$n_1 = 265 \frac{1}{min};\ n_2 = 375 \frac{1}{min}$$

The product of the number of different parameters is 2·2·6=24, meaning that 24 different surface sections need to be created to measure the surface roughness after diamond burnishing. For this purpose, four test specimens were manufactured. After preliminary turning, each specimen was prepared with six cylindrical surfaces suitable for diamond burnishing. These were produced in the workshop of the Institute of Manufacturing Science at the University of Miskolc. The parameter combinations are summarized in Table 1, grouped by specimen and numbered in groups of six.

Table 1. Technological parameters of the diamond burnishing process

Serial Nr.	$\boldsymbol{f}\ \left[\frac{\boldsymbol{mm}}{\boldsymbol{rev}}\right]$	$\boldsymbol{n}\ \left[\frac{\boldsymbol{1}}{\boldsymbol{min}}\right]$	$\boldsymbol{F_v}\ (\boldsymbol{N})$
1-1	0.05	265	120
1-2	0.05	265	100
1-3	0.05	265	80
1-4	0.05	265	60
1-5	0.05	265	40
1-6	0.05	265	20
2-1	0.1	265	120
2-2	0.1	265	100
2-3	0.1	265	80
2-4	0.1	265	60
2-5	0.1	265	40
2-6	0.1	265	20
3-1	0.05	375	120
3-2	0.05	375	100
3-3	0.05	375	80
3-4	0.05	375	60
3-5	0.05	375	40
3-6	0.05	375	20
4-1	0.1	375	120
4-2	0.1	375	100

4-3	0.1	375	80
4-4	0.1	375	60
4-5	0.1	375	40
4-6	0.1	375	20

The test specimens were made from grade 1.4307 austenitic stainless chromium-nickel steel, whose material properties are as follows: yield strength $R_{p0,2} \geq 210\,MPa$, tensile strength $R_m = 520 - 700\,MPa$, elongation at break $A \geq 45\%$, density $\rho = 7.9\,kg/dm^3$, and hardness $160 - 190\,HB$.

In terms of chemical composition, it consists of 66.8–71.3% iron, ≤0.03% carbon, 1% silicon, 2% manganese, 0.045% phosphorus, 0.015% sulfur, ≤0.11% nitrogen, 17.5–19.5% chromium, and 8–10.5% nickel.

The technical drawing of the test specimen is shown in Figure 4.

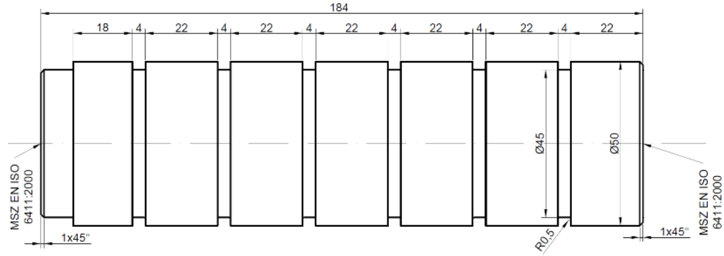

Figure 4. Technical drawing of the test specimen

EU- 400-01 type lathe, and the process conditions are illustrated in Figure 5.

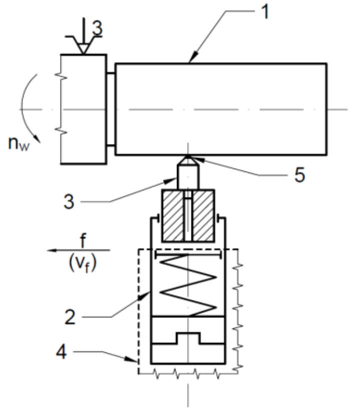

Figure 5. Schematic of the diamond burnishing process [17]

During the research, surface roughness was analysed using several indicators, including 2*D* roughness parameters [17], 3*D* surface roughness values [19], and the

2*D* and 3*D* characteristics of the Abbott-Firestone curves [20], which have already been described in detail in my previous studies.

Surface roughness measurements were carried out using an AltiSurf 520 roughness measurement device, and the results were analysed using the AltiMap software provided with the instrument. Both are in the metrology laboratory of the Institute of Manufacturing Science at the University of Miskolc.

To analyse the characteristics of the Abbott-Firestone curves, we used K-coefficients [20, 21], calculated using Equations (8–13). These equations provide percentage values representing the distribution of the surface profile zones, offering a meaningful comparison of their relevance. For example, Equation (8) shows the proportion of the core roughness within the total 2D roughness profile:

$$K_{Rk} = \frac{R_k}{R_k + R_{pk} + R_{vk}} \quad (8) \qquad K_{Rpk} = \frac{R_{pk}}{R_k + R_{pk} + R_{vk}} \quad (9)$$

$$K_{Rvk} = \frac{R_{vk}}{R_k + R_{pk} + R_{vk}} \quad (10) \qquad K_{Sk} = \frac{S_k}{S_k + S_{pk} + S_{vk}} \quad (11)$$

$$K_{Spk} = \frac{S_{pk}}{S_k + S_{pk} + S_{vk}} \quad (12) \qquad K_{Svk} = \frac{S_{vk}}{S_k + S_{pk} + S_{vk}} \quad (13)$$

3. Evaluation of the research results

To evaluate the results, we first present the calculated values, which are summarized in Table 2. The table lists the technological parameters – feed rate and burnishing force – alongside the calculated burnishing speed, power, and the carbon dioxide emissions associated with each machining operation.

Table 2. Calculated data for diamond burnishing

Serial Nr.	$f\ \left[\frac{mm}{rev}\right]$	$v_v\ \left[\frac{m}{s}\right]$	$n\ \left[\frac{1}{min}\right]$	$F_v\ (N)$	$P\ (W)$	$CE\ (g)$
1-1	0.05	0.6938	265	120	8.33	189.93
1-2	0.05	0.6938	265	100	6.94	158.27
1-3	0.05	0.6938	265	80	5.55	126.62
1-4	0.05	0.6938	265	60	4.16	94.96
1-5	0.05	0.6938	265	40	2.78	63.31
1-6	0.05	0.6938	265	20	1.39	31.65
2-1	0.1	0.6938	265	120	8.33	94.96
2-2	0.1	0.6938	265	100	6.94	79.14
2-3	0.1	0.6938	265	80	5.55	63.31
2-4	0.1	0.6938	265	60	4.16	47.48
2-5	0.1	0.6938	265	40	2.78	31.65
2-6	0.1	0.6938	265	20	1.39	15.83
3-1	0.05	0.9817	375	120	11.78	189.93
3-2	0.05	0.9817	375	100	9.82	158.27

3-3	0.05	0.9817	375	80	7.85	126.62
3-4	0.05	0.9817	375	60	5.89	94.96
3-5	0.05	0.9817	375	40	3.93	63.31
3-6	0.05	0.9817	375	20	1.96	31.65
4-1	0.1	0.9817	375	120	11.78	94.96
4-2	0.1	0.9817	375	100	9.82	79.14
4-3	0.1	0.9817	375	80	7.85	63.31
4-4	0.1	0.9817	375	60	5.89	47.48
4-5	0.1	0.9817	375	40	3.93	31.65
4-6	0.1	0.9817	375	20	1.96	15.83

We analysed the measured surface roughness data using diagrams. The 2*D* surface roughness metrics are shown in Figure 6. In subfigure a) the average roughness, in b) the root mean square roughness, in c) the ten-point mean roughness, and in d) the maximum roughness depth is plotted on the vertical axis, with carbon dioxide emissions on the horizontal axis.

We used different colour codes to represent combinations of feed rate and burnishing speed. Since two types of feed rates and spindle speeds were combined, four parameter combinations were examined. We fitted second-degree polynomials to the data points, and the reliability of these trendlines is indicated by the R^2 values shown in the top right corner of each graph.

To support the analysis, we also added data labels. Each point shows the applied burnishing force and a calculated value – CE(%) – which expresses the relative reduction in carbon dioxide emissions. The formula for CE(%) is given by Equation (12):

$$CE(\%) = \left(1 - \frac{CE_{calculated}}{CE_{max}}\right) 100\ [\%] \qquad (12)$$

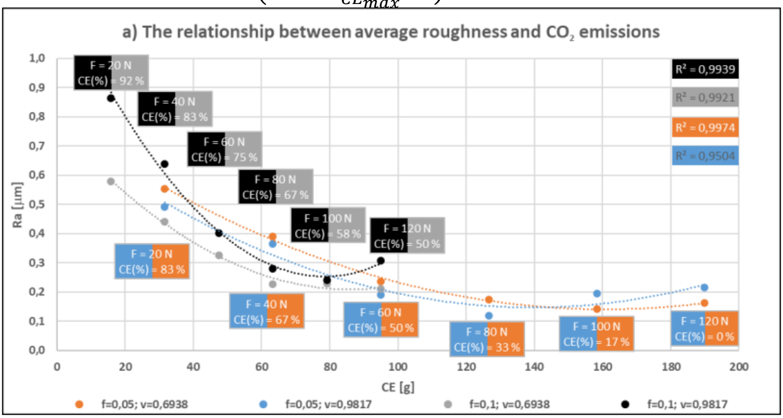

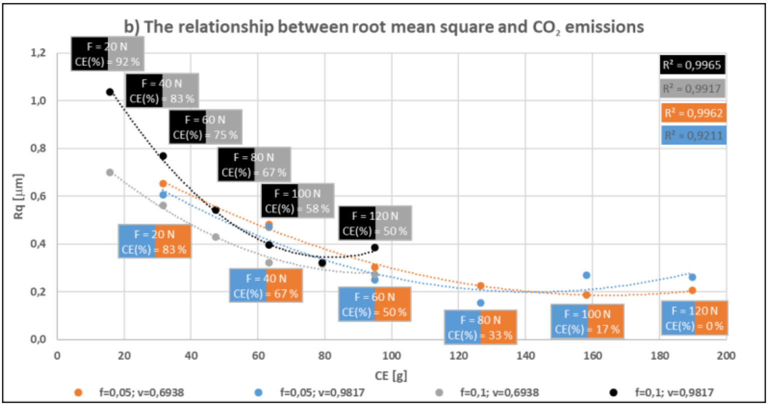
b) The relationship between root mean square and CO2 emissions
Rq [µm]
CE [g]
F = 20 N CE(%) = 92 %
F = 40 N CE(%) = 83 %
F = 60 N CE(%) = 75 %
F = 80 N CE(%) = 67 %
F = 100 N CE(%) = 58 %
F = 120 N CE(%) = 50 %
F = 20 N CE(%) = 83 %
F = 40 N CE(%) = 67 %
F = 60 N CE(%) = 50 %
F = 80 N CE(%) = 33 %
F = 100 N CE(%) = 17 %
F = 120 N CE(%) = 0 %
R² = 0,9965
R² = 0,9917
R² = 0,9962
R² = 0,9211
f=0,05; v=0,6938
f=0,05; v=0,9817
f=0,1; v=0,6938
f=0,1; v=0,9817

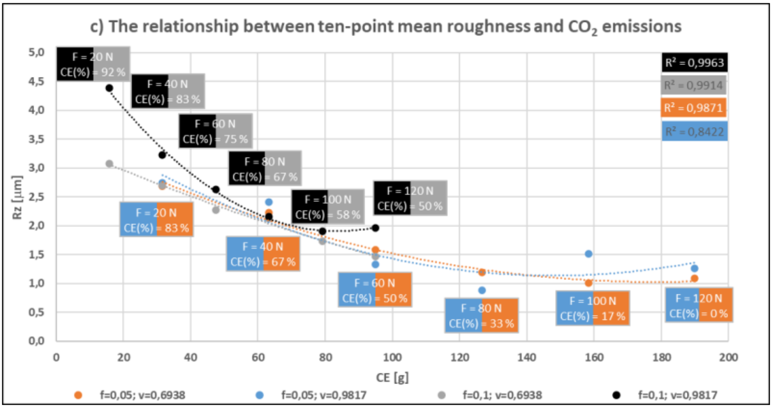
c) The relationship between ten-point mean roughness and CO2 emissions
Rz [µm]
CE [g]
F = 20 N CE(%) = 92 %
F = 40 N CE(%) = 83 %
F = 60 N CE(%) = 75 %
F = 80 N CE(%) = 67 %
F = 100 N CE(%) = 58 %
F = 120 N CE(%) = 50 %
F = 20 N CE(%) = 83 %
F = 40 N CE(%) = 67 %
F = 60 N CE(%) = 50 %
F = 80 N CE(%) = 33 %
F = 100 N CE(%) = 17 %
F = 120 N CE(%) = 0 %
R² = 0,9963
R² = 0,9914
R² = 0,9871
R² = 0,8422
f=0,05; v=0,6938
f=0,05; v=0,9817
f=0,1; v=0,6938
f=0,1; v=0,9817

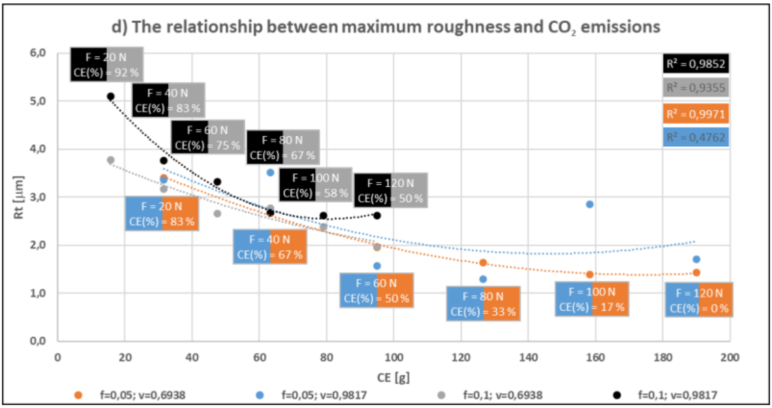
d) The relationship between maximum roughness and CO2 emissions
Rt [µm]
CE [g]
F = 20 N CE(%) = 92 %
F = 40 N CE(%) = 83 %
F = 60 N CE(%) = 75 %
F = 80 N CE(%) = 67 %
F = 100 N CE(%) = 58 %
F = 120 N CE(%) = 50 %
F = 20 N CE(%) = 83 %
F = 40 N CE(%) = 67 %
F = 60 N CE(%) = 50 %
F = 80 N CE(%) = 33 %
F = 100 N CE(%) = 17 %
F = 120 N CE(%) = 0 %
R² = 0,9852
R² = 0,9355
R² = 0,9971
R² = 0,4762
f=0,05; v=0,6938
f=0,05; v=0,9817
f=0,1; v=0,6938
f=0,1; v=0,9817

Figure 6. Relationship between 2D surface roughness parameters and carbon dioxide emissions

To interpret the graphs, we divided the emission value of each data point by the maximum emission value and then subtracted this ratio from one. This yielded the percentage reduction in emissions compared to the worst-case scenario. For the highest emission value (CE=189,93 g), the reduction is naturally 0%. Moving leftward along the horizontal axis – toward zero – the level of emission reduction increases.

Some data points appear in pairs, as similar emission values were observed for different tests with identical feed force ratios. For better clarity, we used gradient shading (black–gray and blue–orange) to distinguish these overlapping points.
Since all subfigures exhibit similar trends, we can confidently state that the conclusions are valid for all types of surface roughness parameters. When using a lower feed rate (represented by orange and blue data points), the trendlines are more elongated, indicating longer processing times and, consequently, higher carbon dioxide emissions. Each of the four trendlines exhibits a parabolic minimum, which appears around 80-100 *N* of burnishing force. Applying forces above this range is not recommended, as it leads to worsening surface quality and increased emissions due to the higher power requirement.

At the same time, surface quality was best achieved using the lower feed rate. However, we found that favourable results can also be achieved with higher feed rates, depending on manufacturing requirements. If ultra-smooth surface quality is not mandatory, adjusting technological parameters may lead to a 60–70% reduction in energy consumption and emissions, while also shortening the machining time. In this way, two common optimization objectives – minimizing energy consumption and machining time – can be achieved simultaneously.

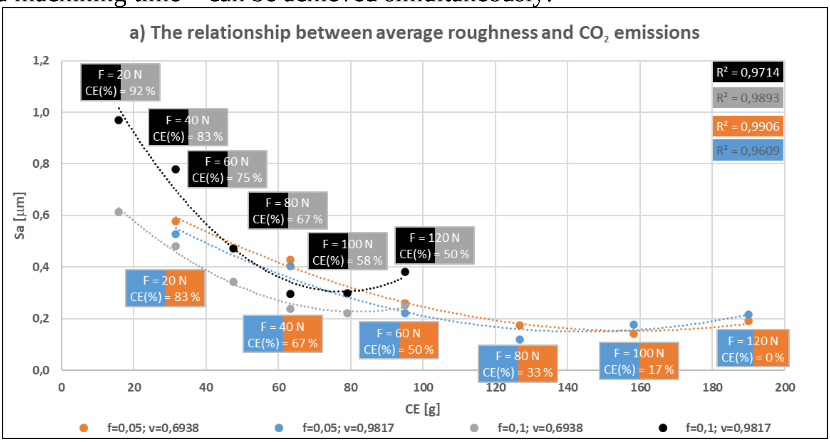

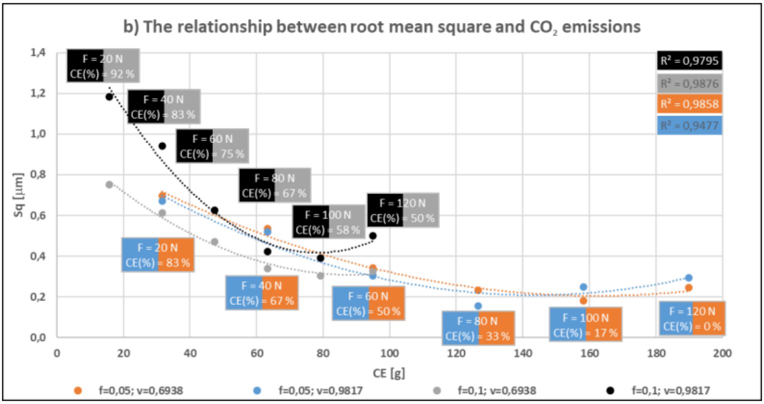
b) The relationship between root mean square and CO2 emissions
Sq [µm]
CE [g]
R² = 0,9795
R² = 0,9876
R² = 0,9858
R² = 0,9477
f=0,05; v=0,6938
f=0,05; v=0,9817
f=0,1; v=0,6938
f=0,1; v=0,9817

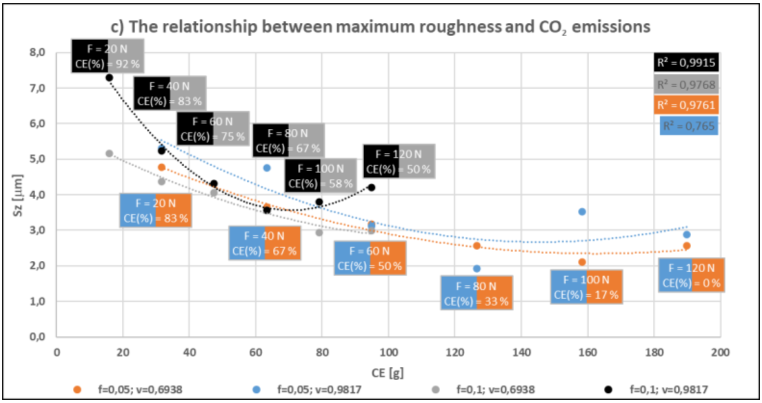
c) The relationship between maximum roughness and CO2 emissions
Sz [µm]
CE [g]
R² = 0,9915
R² = 0,9768
R² = 0,9761
R² = 0,765
f=0,05; v=0,6938
f=0,05; v=0,9817
f=0,1; v=0,6938
f=0,1; v=0,9817

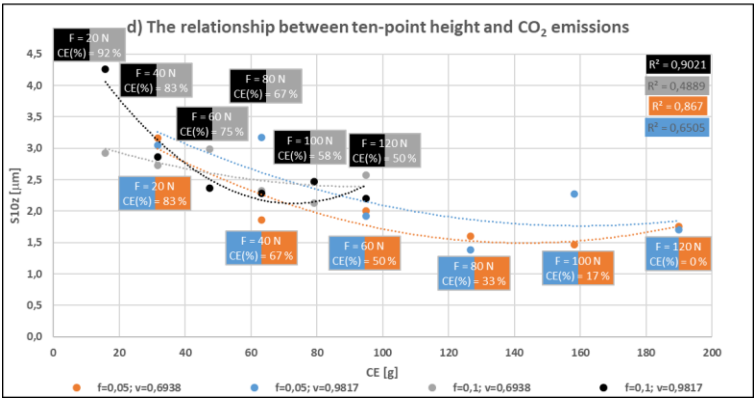
d) The relationship between ten-point height and CO2 emissions
S10z [µm]
CE [g]
R² = 0,9021
R² = 0,4889
R² = 0,867
R² = 0,6505
f=0,05; v=0,6938
f=0,05; v=0,9817
f=0,1; v=0,6938
f=0,1; v=0,9817

Figure 7. Relationship between 3D surface roughness parameters and carbon dioxide emissions

Figure 7 illustrates the 3*D* surface roughness metrics. Subfigure a) presents the arithmetic mean height, b) the root mean square height, c) the maximum height, and d) the ten-point height, all plotted against carbon dioxide emissions. The structure and interpretation of the graphs are consistent with the 2*D* case, and the previously drawn conclusions also apply here.

In the final part of our study, we analysed the material ratio curve parameters – using a different approach due to the unique nature of these metrics. Figure 8 presents these characteristics for both 2*D* and 3*D* profiles, in relation to carbon dioxide emissions.

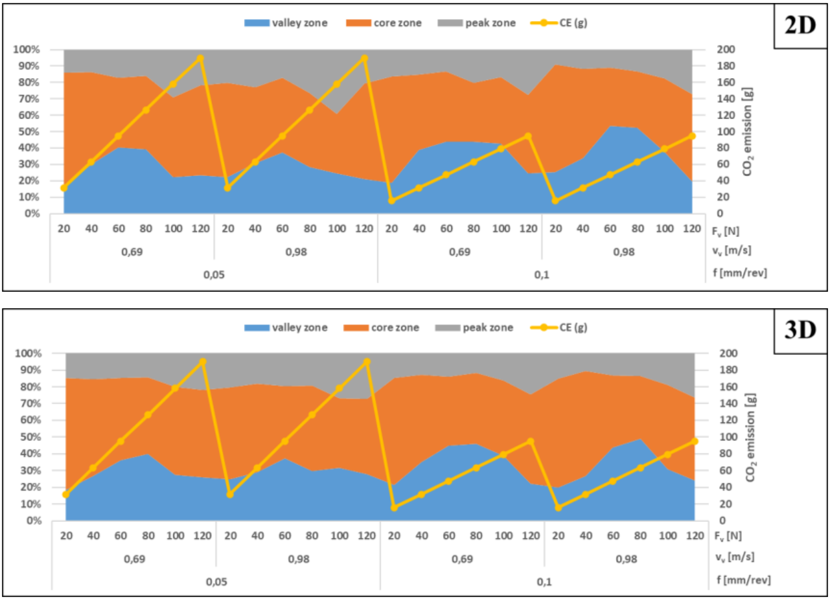

Figure 8. Relationship between material ratio curve parameters and carbon dioxide emissions

Both graphs were prepared using the same methodology. Based on the previously calculated *K* coefficients (according to Equations 8–13), we plotted the relative proportions of the profile zones – for all combinations of feed rate, burnishing speed, and burnishing force. On the secondary axis, we included the carbon dioxide emission value corresponding to each combination. The figures can be interpreted as four separate diagrams representing the four different feed–speed combinations, each with varying burnishing forces.

The goal of diamond burnishing is to reduce the proportion of the peak zone – corresponding to the material that wears off during running-in – to maintain or increase the valley zone, which determines lubricant retention, and to increase or retain the core zone, which bears most of the load.

We observed that the proportion of the peak zone increases at both the lowest and highest applied forces, while the valley zone proportion is at its minimum in these cases – thus these parameter settings should be avoided. With higher feed rates, the maximum valley zone proportion becomes clearly visible, while the peak zone reaches its minimum, indicating optimal tribological performance.

Considering that higher feed rates also proved advantageous in terms of emission reduction and shorter machining time, we recommend using higher feed rates combined with higher burnishing speeds and a burnishing force between 60–80 *N* for optimal results.

4. Summary

First, we reviewed the current state of research related to carbon dioxide emissions and its representation in the literature. Based on a selected method, we presented how CO_2 emissions generated during diamond burnishing can be quantified. Following the calculation, we introduced the technological parameters applied in the machining process, the test specimens on which surface roughness was measured after diamond burnishing, and several additional calculations necessary for data evaluation. Similar trends were observed for both 2*D* and 3*D* surface roughness indicators. It was found that for each combination of feed rate and burnishing speed, a minimum point could be identified on the resulting parabola, beyond which surface roughness no longer decreased. Therefore, applying higher burnishing forces beyond this point is not recommended, as it not only deteriorates surface quality but also increases carbon dioxide emissions due to higher power consumption. Furthermore, we determined that if achieving the best possible surface quality is not a strict requirement, it is worth considering the modification of technological parameters. This can significantly reduce energy consumption and CO_2 emissions – by as much as 60–70% – and even shorten machining times, all while improving the energy and eco-efficiency of the process. In this way, two commonly pursued objective functions – minimization of machining time and energy consumption – can be addressed simultaneously.

Regarding the analysis of the Abbott-Firestone curves, it was demonstrated that the proportion of the peak zone increases at both the lowest and highest burnishing forces, while the valley zone reaches its minimum at these values. Thus, these burnishing force values should be avoided. When using a higher feed rate, a clear maximum of the valley zone was observed, which is optimal for lubricant retention, while the peak zone reached its minimum. Considering that previous findings also identified higher feed rates as optimal from both CO_2 emission and machining time perspectives, it is recommended to choose this setting in the proposed parameter combination, along with higher burnishing speeds and a burnishing force in the range of 60–80 *N*.

References: **1**. *M. Tóth:* Károsanyag-kibocsátás elemzése szikragyújtású motoron megújuló komponenseket tartalmazó tüzelőanyagok használata esetén motorfékpadi környezetben, in OGÉT 2024 - XXXII. Nemzetközi Gépészeti Konferencia, 2024, pp. 446–451. **2**. *Xin Yao, Wei Yan, Hua Zhang, .Zhigang Jiang, .Shuo Zhu*: A Framework for Carbon Emission Quantification of Mechanical Machining Process Based on IoT and MEFA, IFAC-PapersOnLine, Volume 53, Issue 5, 2020, pp. 25–30, ISSN 2405-8963, https://doi.org/10.1016/j.ifacol.2021.04.079. **3**. *IEA (2024):* CO_2 Emissions in 2023, IEA, Paris https://www.iea.org/reports/co2-emissions-in-2023, Licence: CC BY 4.0. **4**. *Ding, Hui & Guo, Dengyue & Cheng, Kai & Cui, Qi.*: An investigation on quantitative analysis of energy consumption and carbon footprint in the grinding process. Proceedings of the Institution of Mechanical Engineers, Part B: Journal of Engineering Manufacture. 228. 950–956. 10.1177/0954405413508280. **5**. *Dahmus J and Gutowski T.*: An environmental analysis of machining. In: 2004 ASME International Mechanical Engineering Congress (IMECE) and RD&D Expo, Anaheim, CA, 13–19 November 2004, pp.1–10. New York: ASME. **6**. *Tridech S and Cheng K.*: Low carbon manufacturing: characterisation, theoretical models and implementation. Int J of Man Res 2011; 6(2): 110–121. **7.** *Li W and Kara S.*: An empirical model for predicting energy consumption of manufacturing processes: a case of turning process. Proc IMechE, Part B: J Engineering Manufacture 2011; 225(9): 1636–1646. **8**. *Dietmair A and Verl A.*: A generic energy consumption model for decision making and energy efficiency optimisation in manufacturing. Int J Sustain Eng 2009; 2(2): 123–133. **9**. *J. Jeswiet and S. Kara*: Carbon emissions and CES in manufacturing, CIRP Annals—Manufacturing Technology, vol. 57, no. 1, pp. 17–20, 2008. **10.** *Y.-C.Choi and P. Xirouchakis*: Aproduction planning in highly automated manufacturing system considering multiple process plans with different energy requirements, The International Journal of AdvancedManufacturing Technology, vol. 70, no. 5–8, pp. 853–867, 2014. **11**. *K. Fang, N. Uhan, F. Zhao, and J. W. Sutherland*: A newapproach to scheduling in manufacturing for power consumptionand carbon footprint reduction, Journal of ManufacturingSystems, vol. 30, no. 4, pp. 234–240, 2011. **12**. *A. Laurent, S. I. Olsen, and M. Z. Hauschild*: Carbon footprintas environmental performance indicator for the manufacturingindustry, CIRP Annals-Manufacturing Technology, vol. 59, no.1, pp. 37–40, 2010. **13**. *C. Herrmann and S. Thiede*, Process chain simulation tofoster energy efficiency in manufacturing, CIRP Journal of Manufacturing Science and Technology, vol. 1, no. 4, pp. 221–229, 2009. **14**. *C. B. Li, Y. Tang, L. G. Cui, and P. Y. Li*, A quantitative approach to analyze carbon emissions of CNC-basedmachining systems, Journal of Intelligent Manufacturing, 2013. **15.** https://ember-climate.org/data-catalogue/yearly-electricity-data/ (2024. 12. 12.) **16**. *Hannah Ritchie, Pablo Rosado and Max Roser*: “Energy”. Data adapted from Ember, Energy Institute. Retrieved from https://ourworldindata.org/grapher/carbon-intensity-electricity (2024. 12. 12.) **17**. *Varga, G., Smolnicki, S., Babič, M., Caesarendra, W.*: Energy Efficiency Analysis When Grinding and Diamond Burnishing of Components, In: Gençyılmaz, M. Güneş; Durakbasa, Numan M. (ed.-s.) Towards Industry 5.0 : Selected Papers from ISPR2022, Cham, Svájc : Springer International Publishing (2023) pp. 378–396. **18**. Coefficient of Friction Equation and Table Chart, Engineers Edge: https://www.engineersedge.com/coeffients_of_friction.htm% 20 (2024. 12. 13.) **19**. *S. Szilárd and V. Gyula*: Energy efficiency study of diamond burnishing using 3*D* surface roughness parameters, in MECHATRONIKA, VÝROBNÁ TECHNIKA, DIGITÁLNY PODNIK: najnovšie úspechy, výzvy, trendy, 2023, pp. 47–57. **20**. *S. Smolnicki and G. Varga*: Analysis of the Abbott-Firestone curve on a diamond-burnished surface, Cutting and tool in technological systems, vol. 100, pp. 119–138, 2024. **21**. *M. Tomov, P. Karolczak, H. Skowronek, P. Cichosz, M. Kuzinovski*: Mathematical Modelling of Core Roughness Depth During Hard Turning. In: *Królczyk, G., Niesłony, P., Królczyk, J. (eds)* Industrial Measurements in Machining. IMM 2019. Lecture Notes in Mechanical Engineering. Springer, Cham. 2020. https://doi.org/10.1007/978-3-030-49910-5_1

Сілард Смольницькі, Дьюла Варга, Мішкольц, Угорщина

АНАЛІЗ ШОРСТКОСТІ ПОВЕРХНІ ПРИ АЛМАЗНОМУ ВИГЛАДЖУВАННІ У ВЗАЄМОЗВ'ЯЗКУ З ВИКИДАМИ ВУГЛЕКИСЛОГО ГАЗУ

Анотація. *У сфері механічної переробки викиди вуглекислого газу також можуть бути значними. Тому важливо визначити оптимальні процеси з правильними параметрами процесу, які допоможуть зменшити викиди CO_2. Очевидно, що низьковуглецеве виробництво стало ключовим очікуванням у промисловості. Тому кількісний аналіз споживання енергії та викидів CO_2 у виробничих процесах є важливим. Саме це веде нас від наукового розуміння ефективного виробництва до промислового впровадження. Ґрунтуючись на обраному методі, ми представили, як можна кількісно оцінити викиди CO_2, що утворюються під час алмазного вигладжування. За підсумками розрахунку ми представили технологічні параметри, що застосовуються в процесі механічної обробки, випробувальні зразки, на яких вимірювалася шорсткість поверхні після алмазного вигладжування, і кілька додаткових розрахунків, необхідних для оцінки даних. Аналогічні тенденції спостерігалися як для 2D, так і для 3D показників шорсткості поверхні. Було встановлено, що для кожної комбінації величини подачі і швидкості вигладжування на отриманій параболі можна визначити мінімальну точку, за межами якої шорсткість поверхні вже не зменшується. Тому не рекомендується застосовувати більш високі сили вигладжування за межами цієї точки, оскільки це не тільки погіршує якість поверхні, але й збільшує викиди вуглекислого газу через більш високе споживання енергії. Крім того, ми визначили, що якщо досягнення найкращої якості поверхні не є суворою вимогою, варто розглянути можливість модифікації технологічних параметрів. Це може значно зменшити споживання енергії та викиди CO_2 – на 60–70% – і навіть скоротити час обробки, одночасно підвищуючи енергетичну та екологічну ефективність процесу. Таким чином, можна одночасно вирішити дві загальні цільові функції - мінімізацію часу обробки і споживання енергії. Щодо аналізу кривих Еббота-Файрстоуна було продемонстровано, що частка пікової зони зростає як при найнижчій, так і при найвищій силі вигладжування, тоді як зона долини досягає свого мінімуму при цих значеннях. Таким чином, цих значень сили вигладжування слід уникати. При використанні більш високої швидкості подачі спостерігався чіткий максимум зони розжолобка, який є оптимальним для утримання мастила, в той час як зона піку досягала свого мінімуму. Враховуючи, що попередні результати також визначили вищі швидкості подачі як з точки зору викиду CO_2, так і з точки зору часу обробки, рекомендується вибрати цей параметр у запропонованій комбінації параметрів, поряд із вищими швидкостями вигладжування та силою вигладжування в діапазоні 60–80 Н.*

Ключові слова: *енергоефективність; сталий розвиток; вигладжувальне алмазне полірування; обробка поверхні.*